Article:

Clarke, S.D., Fay, S.D., Warren, J.A. et al. (2015) Geotechnical causes for variations in output measured from shallow buried charges. International Journal of Impact Engineering, 86. 274 - 283. ISSN: 0734-743X

https://doi.org/10.1016/j.ijimpeng.2015.08.009

Geotechnical Causes for Variations in Output Measured from Shallow Buried Charges

S.D. Clarke[a,*], S.D. Fay[a,b], J.A. Warren[a,b], A. Tyas[a,b], S.E. Rigby[a], J.J. Reay[b], R. Livesey[c], I. Elgy[c]

[a]*Department of Civil & Structural Engineering, University of Sheffield, Mappin Street, Sheffield, S1 3JD, UK*
[b]*Blastech Ltd, The Sheffeld Bioincubator, 40 Leavy Greave Road, Sheffield, S3 7RD, UK*
[c]*Physical Protection Group, Dstl Porton Down, Salisbury, SP4 0JQ, UK*

Abstract

The role of the geotechnical conditions on the impulse delivered by a shallow buried charge has received much attention in recent times. As the importance of the soil in these events has become better understood, the control over the geotechnical conditions has improved. While previous work has investigated directly the role of geotechnical conditions on the magnitude of the impulse from a buried charge, the current work aims to identify how these same conditions also affect the repeatability of testing using soils. In this paper the authors draw together their work to date for a wide range of different soil types and moisture contents to investigate the variation in output from nominally identical tests. The methodology for the preparation of soil beds and the measurement of impulse is described along with the measured variations in peak and residual deflections of a target plate fixed to the impulse measurement apparatus.

Keywords: Buried charges, Impulse, Geotechnics, Soil, Plate deformation, IEDs

1. Introduction

With the increasing use of buried improvised explosive devices in current conflict zones, a need for a deeper understanding of the role of soil in the resulting explosive events has emerged. Being able to design protective structures to withstand such events, and save lives, depends on

*Tel.: +44 (0) 114 222 5703
Email address: sam.clarke@sheffield.ac.uk (S.D. Clarke)

the accurate assessment of the blast loading produced by the detonation of such shallow-buried explosives. This is a highly complex detonation event, involving the interaction of extremely high-energy shock waves with multiple materials in different phases.

Experimental research into characterising the loading from buried explosives has typically focused on the structural response of a target [1, 2] with the geotechnical conditions prior to detonation being of secondary concern. In more recent studies attention has been given to the geotechnical conditions albeit without a full understanding of their role in the underlying repeatability of the event [3, 4, 5, 6, 7, 8]. As an alternative, the shock-related aspects can be removed altogether by using well controlled small scale laboratory samples loaded by compressed gas [9]. This approach has the drawback of over-simplifying the problem by ignoring the air shock, geometrical and thermal aspects of the loading, and perhaps even more critically concentrating only on the sand throw as the mechanism for impulse transfer.

It is generally accepted that geotechnical properties of the soil surrounding a buried charge are of key importance in determining the variation in output. Significant parameters include; bulk density, moisture content, particle size distribution and burial depth. With so many possible principal variables being present, control of the geotechnical conditions is key to understand the relationships between them and the generated impulse.

The authors have shown previously that by carefully controlling the burial conditions very repeatable impulse data can be obtained (±3% for nominally identical tests [10]). This has enabled parametric studies to be conducted to assess the influence of individual geotechnical parameters on the resulting blast. With careful control during the preparation of the soil beds, variations in density of ±0.2%, and in moisture content of ±0.05-0.1% have been achieved. Previous testing has shown that for a fixed bulk density, an increase in moisture content leads to an increase in generated impulse with all other variables remaining constant [10] (series 'a' reported below). Since the previously published work by the authors, a more comprehensive test series, comprising 77 tests (in total) has been conducted. These tests have incorporated the test modifications reported in [11] which improved the accuracy of the image tracking through the use of LEDs set into the target markers. The aim of the research reported herein was to investigate whether certain soil types and conditions produce more repeatable output when comparing the total impulse generated, and the deformation of the target plate. These outputs were also compared to the outputs from tests conducted using a surrogate mine in a steel pot (Minepot) described in the Allied Engineering Publication on procedures for evaluating the protection level of armoured vehicles (AEP-55) [12]. The use of the Minepot hence removes any of the geotechnical conditions as possible causes for the variations in measured impulse and plate deflections.

2. Geotechnical conditions

Soil is a naturally variable material. As such the achievable degree of control of the geotechnical conditions should be a product of this natural variation. Six soils have been tested in the current research at a range of moisture contents (w = mass of water / *dry* mass of solids) and bulk and dry densities (ρ, ρ_d).

Table 1: Soil types used in the current research

Soil	PSD	w (%)	ρ (Mg/m^3)
Leighton Buzzard 14/25 (LB)	Uniform (0.6-1.18 mm)	0-25	1.5-2.0
Leighton Buzzard 6/14 (2LB)	Uniform (1.18-2.8 mm)	0-25	1.6-2.0
Leighton Buzzard 25B grit (LBF)	Well graded (0.5-5.0 mm)	0-25	1.6-2.0
Sandy gravel (Stanag) [12]	Well graded (0-20 mm)	0-14	1.9-2.2
Red building sand (RBS)	Uniform (0.1-0.5 mm)	25	1.9
Brown laminated silty clay	66% < 0.002 mm	~27	1.93

The soil types tested are given in Table 1 with information on the particle size distribution for each soil type being shown in Fig. 1. Uniform soils have a small range of particle sizes and hence plot as steep lines in Fig. 1 e.g. Leighton Buzzard 14/25 (LB) and 6/14 (2LB) sands. Well graded soils have a large range of particle sizes and plot as shallow lines e.g. ‘Stanag’.

Stanag is the sandy gravel recommended for use in buried charge tests given in the AEP-55 [12], which is itself a testing addenda to NATO standardisation agreement, STANAG 4569 [13]. The Leighton Buzzard sands are renowned in the UK for their well-rounded and uniform nature and have a long history of use in geotechnical testing due to their inherently repeatable nature. Their name comes from the town in which they are quarried. For two of the Leighton Buzzard sand gradings (14/25 (LB) & 25B grit sand (LBF)) the test beds were first compacted to a constant bulk density (series 'a' in Table 2, which indicates how each test series varied). Hence, as the water content increased so the dry density decreased. As the dry density decreases the soil becomes more prone to self weight and vibration induced compaction, so great care must be taken when moving soil containers once prepared. In test series 'b', the dry density was kept constant with increased water content leading to an increased bulk density in each test. There is a natural limit on the moisture content achievable whilst still creating a homogeneous sample. Once this limit is passed the water in the soil matrix settles to the bottom of the soil container creating a fully saturated zone at the base with a partially saturated zone above. This is related to the particle size distribution, with the well graded soils being able to sustain higher moisture contents whilst remaining homogeneous. In the case of the Leighton Buzzard sands this limit was found to be around ≈8% moisture content. In test series 'c' the air void ratio (volume of air / total volume) in the sample was kept constant, leading to a reduction in both bulk and dry densities as the water content increased. As in test series 'a' the soils are prone to self compact once the natural minimum dry density is neared, hence low moisture contents were used. The test series types are summarised in Table 2. Further soil types were also tested using the series 'b' methodology, these included Leighton Buzzard 6/14 sand (2LB), AEP-55 sandy gravel (Stanag), brown laminated silty clay (Clay), and red building sand (RBS). The Leighton Buzzard sands provide an opportunity to investigate the effects of particle scaling and particle size distribution for nominally identical materials. Leighton Buzzard sand can be described as a rounded to well-rounded quartz silica sand shown in Fig. 2(a). The red building sand has a

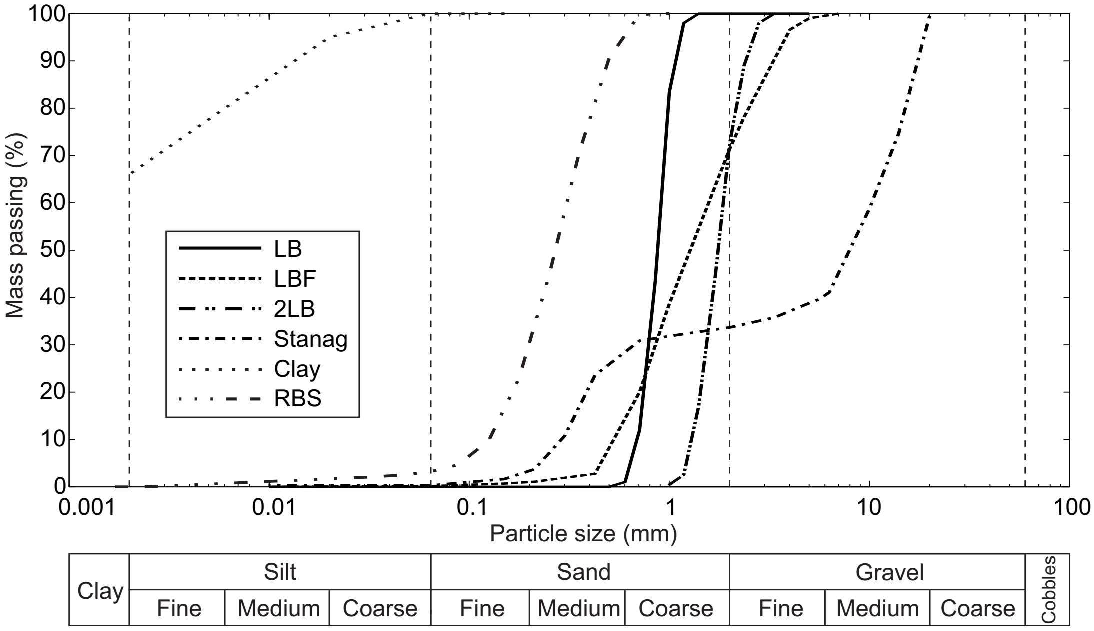

Figure 1: Particle size distribution curves for each soil type

Table 2: Test series conducted

Series	Notes
a	Constant bulk density ($> w$, $< \rho_d$)
b	Constant dry density ($> w$, $> \rho$)
c	Constant air voids ($> w$, $< \rho$, $< \rho_d$)

smaller average particle size and can be described as sub-angular, as shown in Fig. 2(b). For all the soils tested with the exception of the clay, silica is the predominant mineral, giving the soils an identical specific gravity, G_s of 2.65 (Clay $G_s \approx 2.75$).

2.1. Soil preparation

To create repeatable test beds with varying soil types at differing dry densities (and hence levels of compaction), an effectively rigid container was used [10]. The containers were constructed from 30 mm thick rolled mild steel plate formed into a 1000 mm diameter, 750 mm tall cylinder. These dimensions are half scale when compared with the full scale soil beds mandated in AEP-55 [12]. A 25 mm thick mild steel base plate was welded to the base of each cylinder. To be able to control the final conditions of the test beds the initial conditions of the soils were

Table 3: Test plan and achieved geotechnical conditions

Test no.	Soil type	Series	w (%)	ρ (Mg/m^3)	ρ_d (Mg/m^3)
1	2LB	b	2.512	1.633	1.593
2	2LB	b	2.512	1.635	1.595
3	2LB	b	4.993	1.660	1.581
4	2LB	b	4.998	1.679	1.599
5	2LB	b	8.026	1.732	1.603
6	2LB	b	8.085	1.732	1.602
7	2LB	b	24.77	1.990	1.595
8	2LB	b	24.77	1.990	1.595
9	Clay	-	26.50	1.929	1.525
10	Clay	-	26.90	1.925	1.517
11	Clay	-	27.30	1.862	1.463
12	LB	a, b, c	0.100	1.594	1.592
13	LB	a, b, c	0.100	1.593	1.591
14	LB	a, b, c	0.281	1.594	1.589
15	LB	a	2.459	1.596	1.558
16	LB	a	2.470	1.596	1.558
17	LB	a	2.480	1.595	1.556
18	LB	a	4.932	1.595	1.520
19	LB	a	4.998	1.600	1.524
20	LB	a	5.020	1.595	1.519
21	LB	a	7.388	1.598	1.488
22	LB	a	7.446	1.599	1.488
23	LB	a	7.481	1.598	1.486
24	LB	b	2.491	1.643	1.603
25	LB	b	2.491	1.641	1.601
26	LB	b	2.543	1.642	1.601
27	LB	b	4.932	1.670	1.592
28	LB	b	4.943	1.664	1.586
29	LB	b	4.998	1.670	1.591
30	LB	b	8.108	1.733	1.603
31	LB	b	8.108	1.730	1.600
32	LB	b	8.120	1.734	1.604
33	LB	b	24.77	1.990	1.595
34	LB	b	24.77	1.990	1.595
35	LB	b	24.77	1.990	1.595
36	LB	c	1.926	1.557	1.528
37	LB	c	1.978	1.552	1.522
38	LB	c	1.999	1.558	1.527
39	LB	c	3.972	1.509	1.451
40	LB	c	4.037	1.502	1.444
41	LB	c	4.102	1.509	1.450
42	LBF	a, b	0.080	1.600	1.599
43	LBF	a, b	0.080	1.600	1.599
44	LBF	a, b	0.100	1.604	1.602
45	LBF	a	2.470	1.596	1.558
46	LBF	a	2.492	1.603	1.564
47	LBF	a	2.561	1.598	1.558
48	LBF	a	4.833	1.615	1.541
49	LBF	a	4.888	1.613	1.538
50	LBF	a	4.943	1.608	1.532
51	LBF	a	7.411	1.601	1.491
52	LBF	a	7.411	1.605	1.494
53	LBF	a	7.532	1.604	1.492
54	LBF	b	2.480	1.638	1.598
55	LBF	b	2.543	1.631	1.591
56	LBF	b	4.965	1.667	1.588
57	LBF	b	4.965	1.662	1.583
58	LBF	b	8.167	1.730	1.599
59	LBF	b	8.178	1.732	1.601
60	LBF	b	24.77	1.996	1.600
61	LBF	b	24.77	1.990	1.595
62	RBS	-	24.22	1.887	1.519
63	RBS	-	24.22	1.882	1.515
64	RBS	-	24.22	1.881	1.514
65	Stanag	b	0.090	1.937	1.935
66	Stanag	b	0.090	1.928	1.926
67	Stanag	b	4.167	2.006	1.926
68	Stanag	b	4.232	1.999	1.918
69	Stanag	b	8.648	2.088	1.922
70	Stanag	b	8.719	2.097	1.929
71	Stanag	b	11.11	2.148	1.933
72	Stanag	b	11.14	2.133	1.919
73	Stanag	b	14.15	2.198	1.926
74	Stanag	b	14.15	2.201	1.928
75	Minepot	-	-	-	-
76	Minepot	-	-	-	-
77	Minepot	-	-	-	-

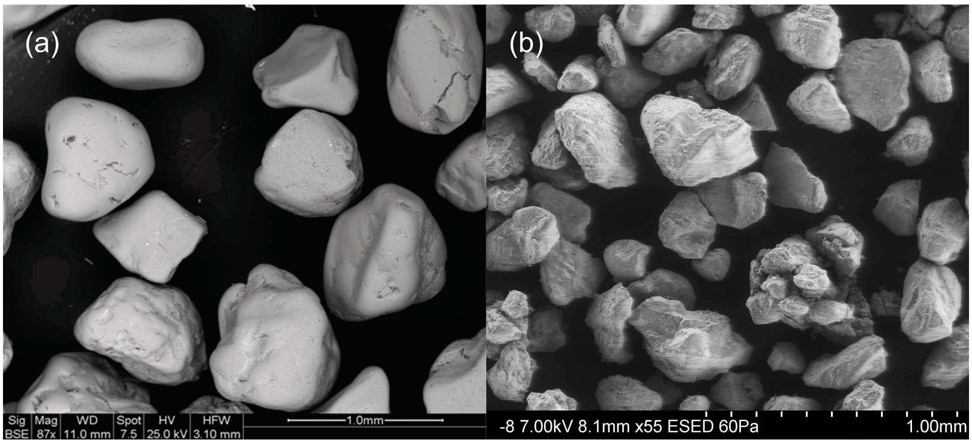

Figure 2: Scanning electron micrograph of (a) Leighton Buzzard sand [14] (b) Red building sand

checked prior to sample preparation. The initial moisture content of each soil was checked, and the mass of water required to achieve the test prescribed water content was calculated. This led to samples being created to within ±0.1% of the target moisture content. Ideally all soils would be initially dry but this introduces complications in the production of repeatable samples with cohesive soils such as clays which require a long period of consolidation.

For the cohesionless soils, the containers were generally filled in 3 stages each of equal mass (the exact mass depends on geotechnical conditions of the test). The soil was weighed as it entered a forced action pan mixer and the correct mass of water added. Mixing continued until the water was evenly distributed; with moisture content then being checked. If the moisture content was confirmed to be within tolerance, the contents of the pan mixer were purged into the soil container taking care to avoid sample loss. Plywood shuttering (cut to the internal diameter of the container) was placed on the surface of the soil and a stiffened steel plate (100 mm clear of the internal diameter) was seated on the timber boards. A vibrating compaction plate (VCP) was placed upon the stiffened steel plate; the soil then being vibrated until it reached its target density. Measurements of the final soil depth were then recorded. The VCP, stiffened steel plate and timber boards are then removed from the container with care such that the soil surface remains undisturbed. This was repeated until the container was filled. In the case of the non

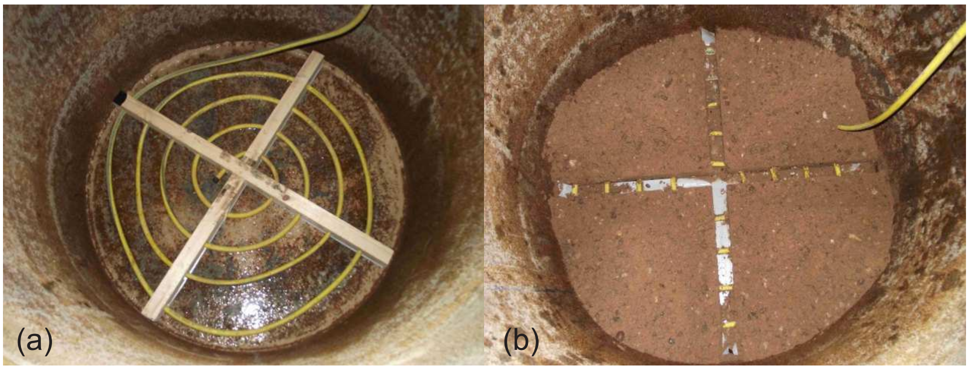

Figure 3: Bottom-up saturation technique (a) spacer present (b) part-filled with spacer removed

saturated soils a cavity was then excavated to accommodate the charge, at the correct burial depth. Excavated material was stored in sealed bags, in order to back fill to the correct density and moisture content.

For the full saturation tests the soil containers were filled using the above procedure to a designated dry density and then saturated from the base [15]. Fig. 3 shows the inside of the steel containers during filling. Any collapse settlement during the saturation process is accounted for in the initial target dry density to achieve the same bulk density in each test. The base saturation is achieved by burying a length of perforated hose, using a timber spacer to achieve an even hose distribution (Fig. 3a). This spacer is then removed once enough soil has been added to secure the hose location (Fig. 3b). The container is then filled in the usual manner with the hose being led up the inner wall to allow for saturation prior to firing. This method of flooding has been found to give a more uniform distribution of moisture content through the soil mass, so long as the flow rate used for saturation is insufficient to cause piping.

For the cohesive tests there are two ways of preparing the soil bed. One method is to reconstitute the soil from a high moisture content slurry under sustained pressure, which leads to a very high degree of control but very long preparation times. The second method is to ‘press in’ the soil containers into a natural clay outcrop, thus testing ‘real’ materials. In the current study the second method was used with the authors sourcing a supplier capable of using heavy plant to force the containers into a uniform outcrop, with the surface being levelled with a wire saw to obtain a relatively undisturbed face. With the second method, the moisture content and density are controlled by the uniformity of the natural outcrop– the variation in the soil beds is recorded in Table 3.

3. Experimental setup

3.1. Test frame

All experimental work was conducted by Blastech Ltd at the University of Sheffield Blast & Impact laboratory, Buxton, UK as part of a research project funded by the UK Defence Science and Technology Laboratory (Dstl). The large test frame fabricated is shown in Fig. 4. The deformable target plate is made from a 12.5 mm thick, 675 mm square mild steel sheet. This was attached to a 675 mm square stiff reaction frame, fabricated from 100 mm thick mild steel, with a circular free span for the target plate of 500 mm diameter. The reaction frame in turn was connected to a 3 m long steel circular hollow section. The resulting system had an overall reaction mass of 1574 kg. The entire reaction mass was allowed to translate freely in the vertical direction after picking up load from the detonation of a buried explosive charge, with up to 800 mm of vertical travel allowed. The upward flight was then arrested either by gravity (if the initial velocity $<\approx 4$ ms^{-1}) or by impact of the interface plate with the lower face of the arrestor plate. As the mass subsequently descends, the lower flange settled onto the upper face of the arrestor plate, where the impact was softened by bushes. Peak and residual deflections of the deformable target plate were measured (§3.4). For the purposes of future numerical analysis, the 12.5 mm thick target plates were attached to the interface plate using 4 timber pegs which are designed to resist minimal loading, thus simplifying the boundary conditions of the plate to that of unrestrained, with the target plate simply bearing directly onto the inner profile of the interface plate. The detached target plate was free to fall into the soil container once the event was over reducing any further deformation from the landing.

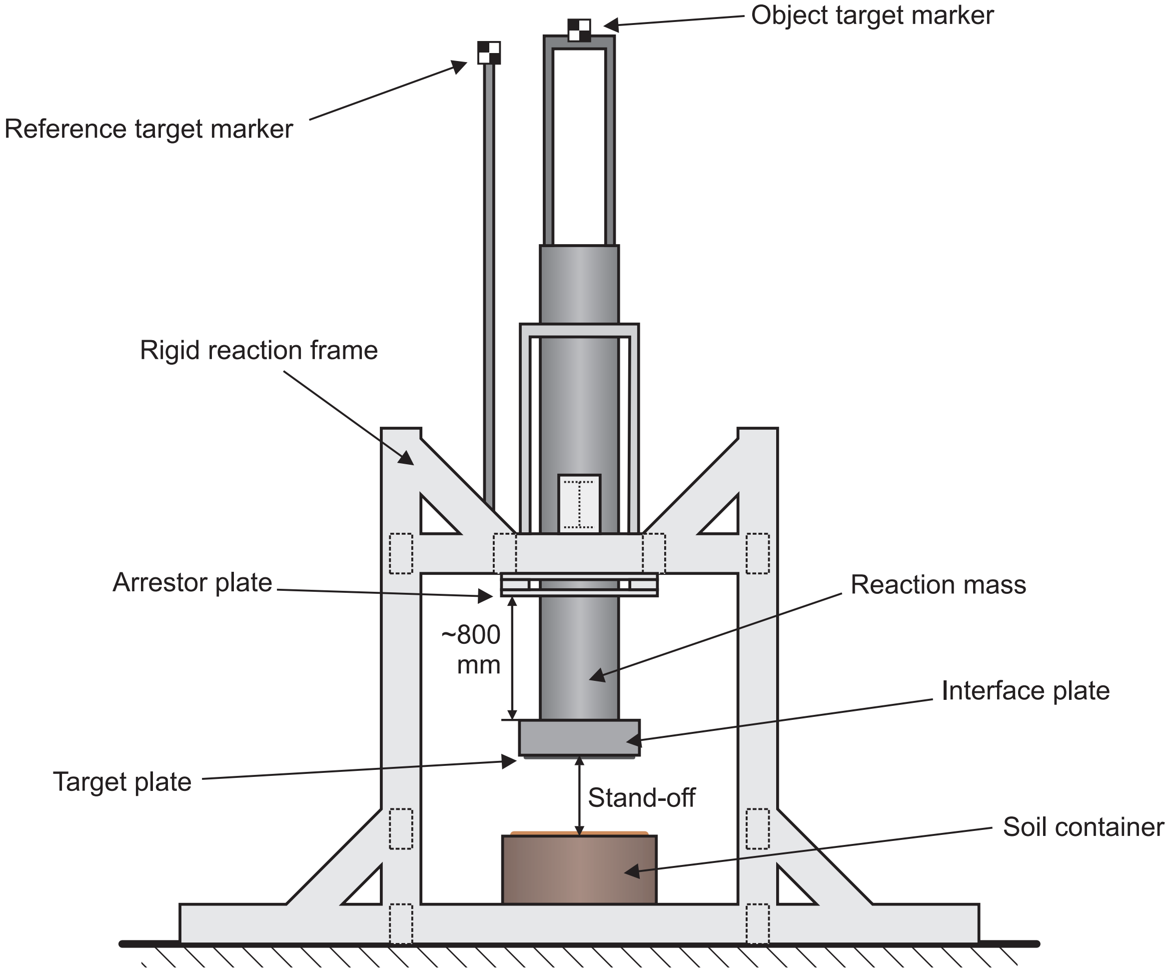

Figure 4: Free-flying mass impulse capture apparatus

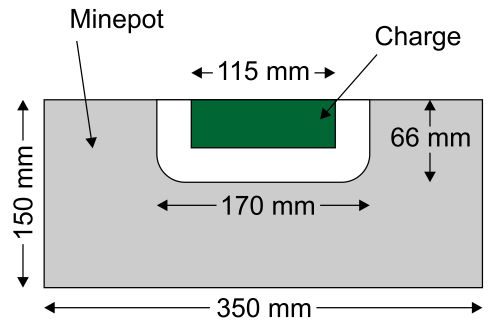

Figure 5: Scaled down surrogate mine in steel pot (Minepot)

3.2. Test configuration

The present work used a half linear scale version of STANAG threat level M2 as given in AEP-55 [12]. The size of the soil container has also been scaled down to emulate the boundary conditions stipulated in AEP-55 with the exception of the boundary being cylindrical rather than rectangular. Due to the physically smaller charges being used (1/2 scale by geometry, 1/8 scale by mass and energy), the Minepot was also scaled down to half scale, Fig. 5. In each test a charge of 625 grams PE4 buried at 50 mm, measured from the soil surface to the top of the charge, was used. The charge was shaped into a 3:1 cylinder as indicated in Fig. 5. The stand-off between the soil surface and the target plate was 137.5 mm in all tests.

3.3. Impulse measurement

In order to measure displacement-time data of the reaction mass, two target markers are attached to the rig (Fig. 4), one to the rigid reaction frame to give a fixed reference, the other attached to the rising mass. Both target markers are raised up on masts to ensure they are not obscured by soil throw during the test. Two high-speed cameras (Dantec Dynamics NanoSense Mk.2, framing at 4000 fps) are used, one to film these target markers and one to film the breakout of the charge and resulting sand throw. An example of the footage from the lower camera is shown in Fig. 6. The lower camera was situated within a reinforced concrete bunker and isolated from any potential air shock vibration.

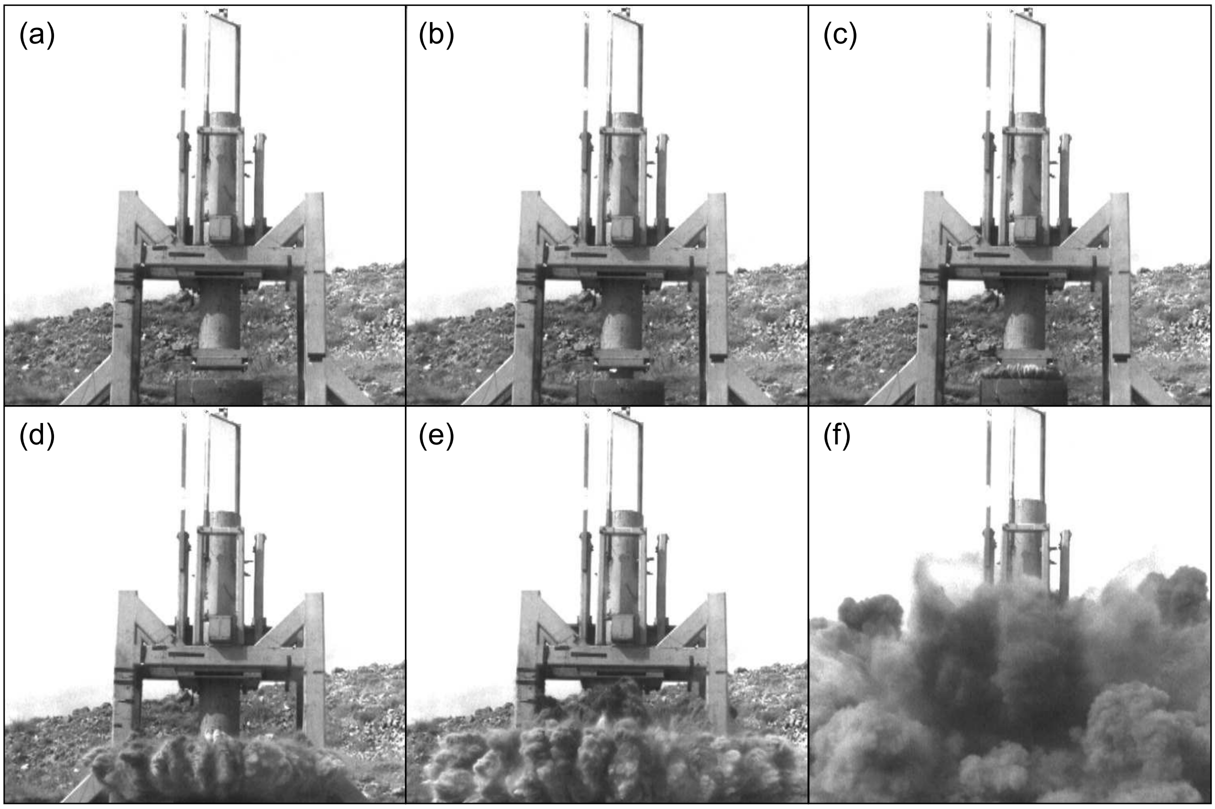

Figure 6: Frames from high speed video of an indicative test; a) pre firing, b) initial vertical throw, c) cloud reaches container edge, d) expansion clearing frame, e) expansion into free air, f) target movement clearly visible from object target marker

The upper camera was situated in protective housing on the bunker roof (at roughly the same height as the target markers), which made it prone to vibration from the air shock, potentially introducing an error into the marker tracking. However, since the excitation is common to both target markers, the error can be minimised by subtracting the motion of the reference target marker from that of the object target marker. Using the relative motion, the displacement-time history for the target can be calculated to which a 4th order polynomial is fitted, an example displacement-time history from the image tracking is shown in Fig. 7. The equivalent initial velocity that would give the same peak rise as seen in the polynomial fit can then be calculated. The velocity calculation assumes the velocity is applied instantaneously with the target mass subsequently free to decelerate under gravity. The initial impulse can then be calculated from knowing the mass and initial velocity [10, 11].

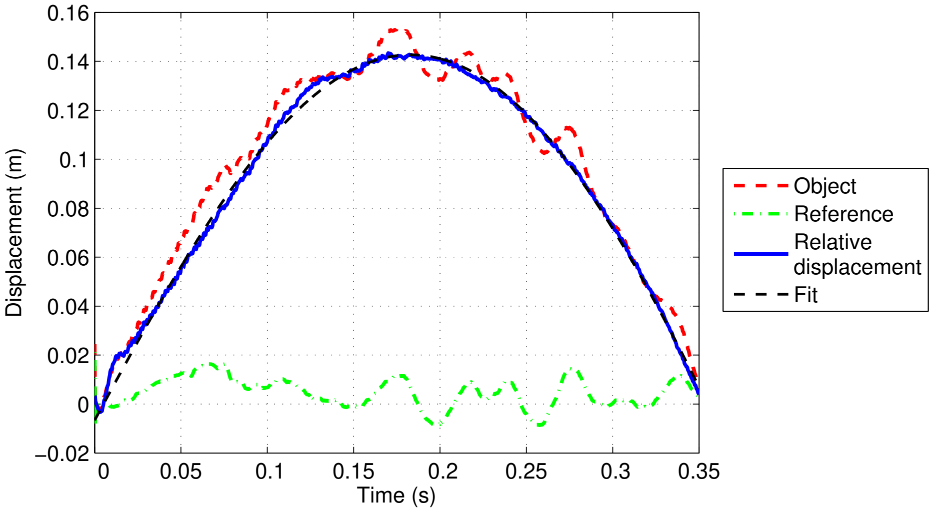

Figure 7: Example displacement-time history of the object and reference target markers with 4th order polynomial curve fit to relative displacement data

3.4. *Deflection measurement*

The peak and residual plate deflections were also recorded. The peak dynamic deformation of the target plate (relative to the interface plate) was accurately measured using a deformable aluminium honeycomb crush block, mounted on a rigid support spanning the 500 mm circular hollow section. The residual deflections were recorded post test once the plate was recovered. These data give a second measure on the ability of a given soil type (or the Minepot) to produce repeatable results.

4. Results

4.1. *Global repeatability*

The focus of this paper is not to directly compare the magnitude of the impulses and deflections generated, but to compare the repeatability of the tests. This has been achieved by normalising all data in a test series by the mean for that test series. The mean-normalised impulse for each test is shown in Fig. 8(a), where the mean-normalised impulse was calculated by dividing the recorded impulse by the mean impulse for the subset of nominally identical tests (see shading in Table 3). The normalised residual and peak plate deflections were calculated in an identical manner and are plotted against test number in Figs. 8(b) and 8(c) respectively.

Fig. 8(a) shows the repeatable nature of the testing with the maximum offset of any data point being test 53 which shows a 0.166 (16.6%) variation from the mean. The likely cause for this variation is the low dry density of the soil combined with a relatively high moisture content making it highly susceptible to self compaction as noted earlier and is a common factor in all 'a' series tests. All the other tests lie within 10% of the mean. From a comparison between Fig. 8(a), (b) and (c) it can be seen that a low variation in impulse does not necessarily lead to equally low variation in recorded deflection. For example LBb shows one of the lowest variations in impulse (SD=0.0112, lower than that of the Minepot, SD=0.0201) yet one of the highest variations in peak deflection (SD=0.0447). The standard deviations for all the individual test soil types for the three measured outputs are given in Table 4.

Table 4: Soil type repeatability

	Standard deviation / soil type									
Output	2LB	Clay	LBa	LBb	LBc	LBFa	LBFb	RBS	Stanag	Minepot
Impulse	0.0124	0.0088	0.0340	0.0112	0.0463	0.0694	0.0371	0.0070	0.0313	0.0201
Residual deflection	0.0354	0.0158	0.0275	0.0350	0.0302	0.0268	0.0236	0.0308	0.0197	0.0072
Peak deflection	0.0243	0.0210	0.0176	0.0447	0.0269	0.0299	0.0171	0.0570	0.0232	0.0114

When the dataset is taken as a whole, the absolute offset of each test from the mean can be plotted against the number of tests within that offset as shown in Fig. 9. This shows that the range of impulses is higher than that of both deflections when considering 100% of the data. This is reflected by the global standard deviations given in Table 5. However, when considering only the closest 80% of data to the mean there is very little variation between the impulse and deflections with 80% of the data lying within ±3.7% of the mean. The variation reduces to ±2.2% when looking at 50% of the data and ±1% when looking at 30%.

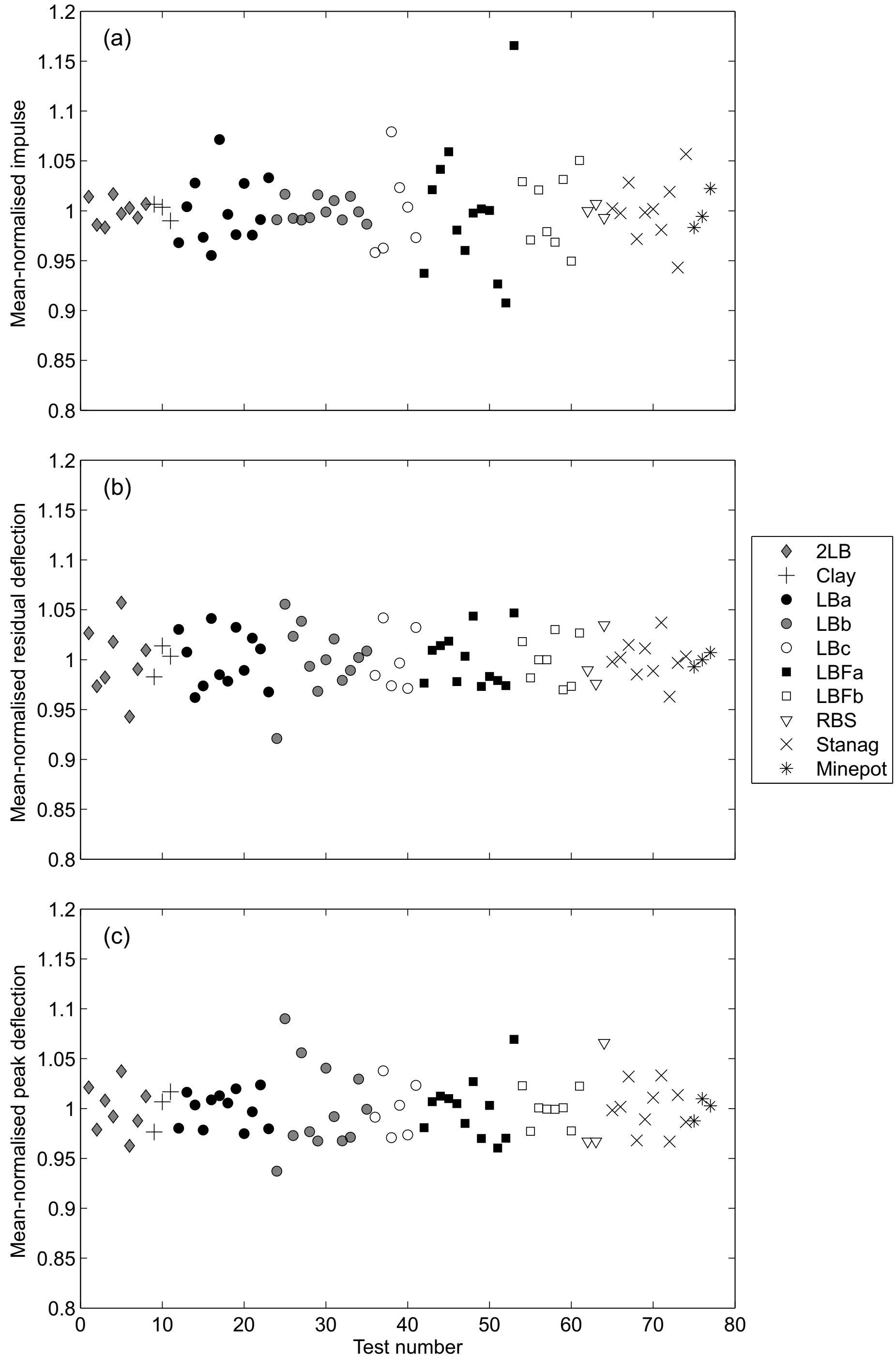

Figure 8: Mean-normalised (a) impulse, (b) residual plate deformation and (c) peak plate deformation for all tests

Table 5: Global repeatability

Output	Standard deviation	
	100%	80%
Impulse	0.0360	0.0174
Peak deflection	0.0275	0.0178
Residual deflection	0.0264	0.0176

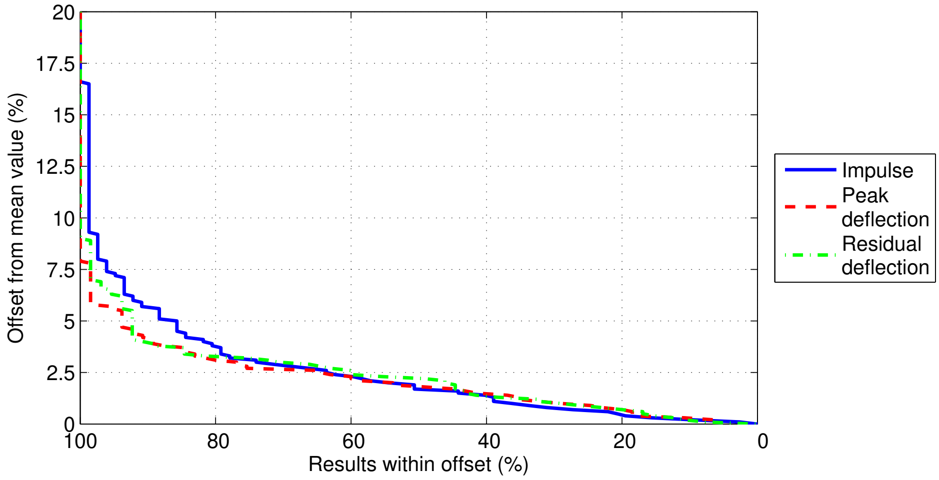

Figure 9: Offset from the mean for all data

4.2. *The effect of bulk density on repeatability*

To identify the trends and to allow for a more in depth comparison of the geotechnical conditions, the data have been re-analysed to give the range (maximum − minimum) of output for each set of repeat tests. This range is then mean-normalised. Thus in the figures presented, each data point represents a sub series of tests (for the Clay this would be tests 9-11). The range has then been plotted against bulk density in Fig. 10. For comparison the normalised range is plotted for the Minepot results (the Minepot is shown as a line as there is no soil present, hence the geotechnical conditions are irrelevant). This indicates that for certain soil types at specific bulk densities it may be possible to achieve a higher repeatability than seen in the Minepot results. In fact, Minepot tests are commonly favoured due their highly repeatable nature. The data presented herein shows that whilst the Minepot standard is repeatable, there are specific soil conditions which may give a more repeatable impulse. Fig. 10(a) shows that the largest variations in impulse are seen in the well graded soils - Stanag (SD=0.0313) and LBFb (SD=0.0371). The LBFb variation was consistently greater than that seen in the Minepot (SD=0.0201). As identified previously the most repeatable impulse data came from the LBb data series (SD=0.0112) which showed consistently less variation than the Minepot. Further statistics can also be used to analyse the data in Fig. 10. Specifically, the correlation using the Spearman rank correlation coefficient r_s, which evaluates how well the relationship between bulk density and the measured outputs can be described using a monotonic function. This indicates a moderate negative correlation between the bulk density of the soil and the variation in impulse (r_s=-0.4504, p=0.0097) and residual deflection (r_s=-0.4406, p=0.0116). The statistical significance of these results is high given the number tests, indicated by the low probability p values. Interestingly the same trends were not seen in the peak deflection data (r_s=-0.0294, p=0.8733) though almost no confidence can be put in this due to the very high p value.

4.3. The effect of moisture content on repeatability

For each soil type shown in Fig. 8, as the test number increases so does the moisture content used in the test. The increasing moisture content makes little difference to the variation in impulse (with the exception of the series ‘a’ tests as discussed earlier), it does however have a marked influence on the deflections seen in certain soil types. This is seen clearest in the LBb tests where is a strong correlation between increasing moisture content and deducing residual deflection range (r_s=-0.7, p =0.2333). It is noted that with a sample size of 4 this is underpowered and would require further testing to gain a statistically significant result. The authors hypothesise that in the LBb tests at saturation increases so does the spatial uniformity of the breakout, this has the effect of delivering the loading to the target plate more uniformly and hence producing repeatable deflections. In well graded soils and low moisture content tests the spatial variability of the loading will give rise to greater variation in the deflections generated.

The mean-normalised outputs have been replotted against bulk density as shown in Fig. 11.

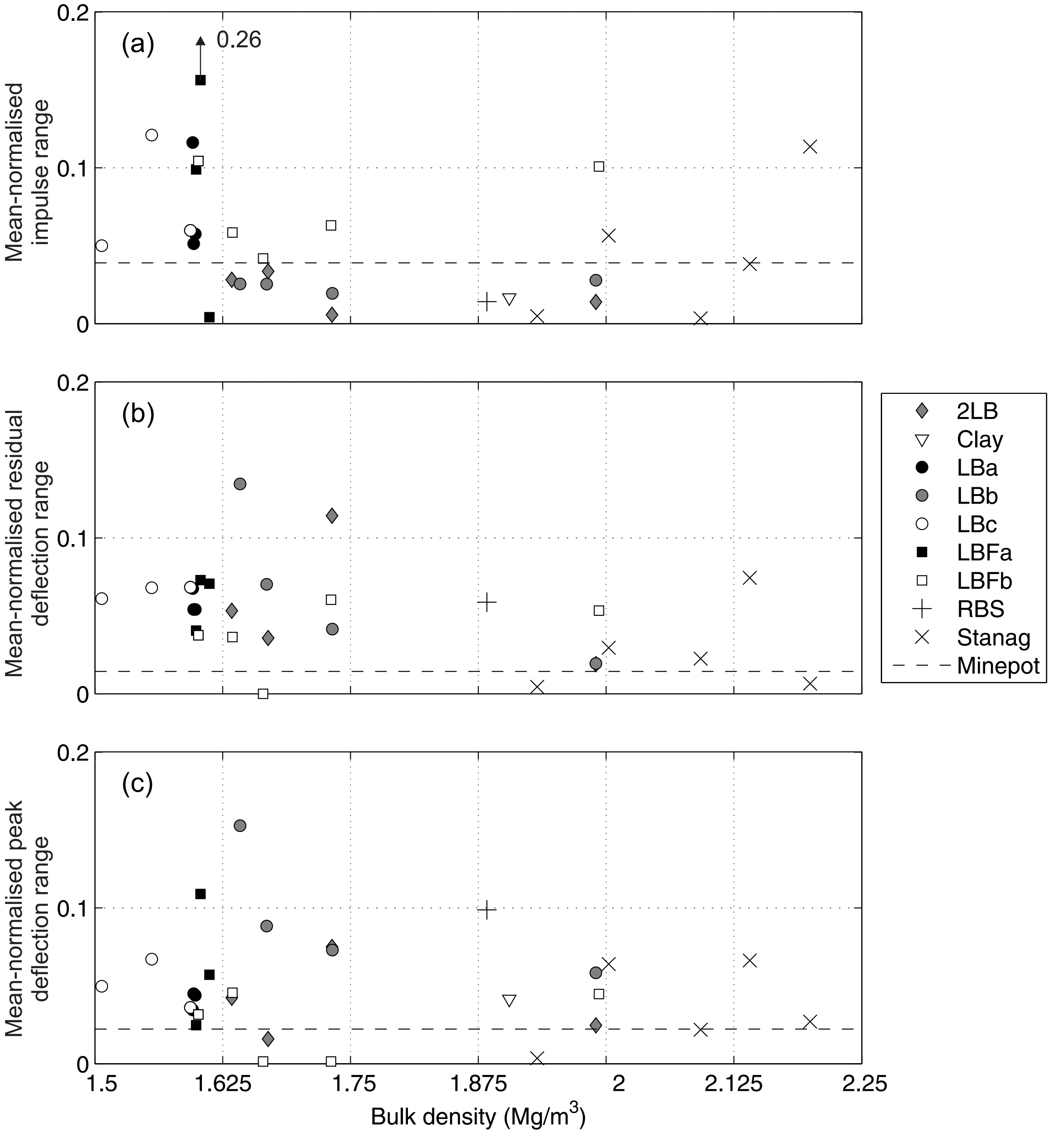

Figure 10: Bulk density versus the mean-normalised range of (a) impulse (b) residual deflection and (c) peak deflection

This shows the same trends as were present in Fig. 10, which is due to the intrinsic linking of moisture content and bulk density. Again, this shows that certain soil types at specific moisture contents it is possible to achieve a higher repeatability than seen in the Minepot results. The fully saturated tests here are easier to identify, sitting at ~25%, the notable exception being the Stanag soil which sits at a moisture content of 14% when fully saturated with a bulk density of 2.2 Mg/m^3. The maximum range of 0.114 (11.4%) for the fully saturated Stanag may at first glance seem large, but this is mainly due to the fact that other soil types / conditions are very repeatable.

4.4. Repeatability of output versus repeatable preparation

It is clear that the geotechnical conditions have a large impact on the repeatability of any proposed testing. With differing soils come variations in both the output of a charge buried within that soil and a varying degree of repeatability of the preparation of the soil bed itself. It can be logically deduced that variations in the density and moisture content of a soil bed should directly impact on the variations in measured output. While this has been shown to be true, there is no direct relationship between the two due to the influence of soil type. With some soils it is hard to achieve repeatable initial conditions, whilst a low variation in output may still be achieved (Clay) and vice versa. This point is illustrated in Fig. 12 which plots the standard deviations of moisture content and bulk density on the two horizontal axes and the range of mean-normalised impulse on the vertical. On the horizontal axes, low values mean that both the moisture content and bulk density are repeatable using the preparation methodologies outlined earlier. This shows that the LBFa series soil conditions were one of the most difficult to consistently prepare (disregarding the natural clay). For the well graded soils such as Stanag and LBFb, whilst the preparation was repeatable, a relatively high degree of impulse variation was generated. The authors hypothesise that the well graded nature of these soils leads to a non-uniform breakout which can give rise to the variations in output measured. For uniform soils such as LBb the breakout is hypothesized to be relatively uniform giving a more repeatable

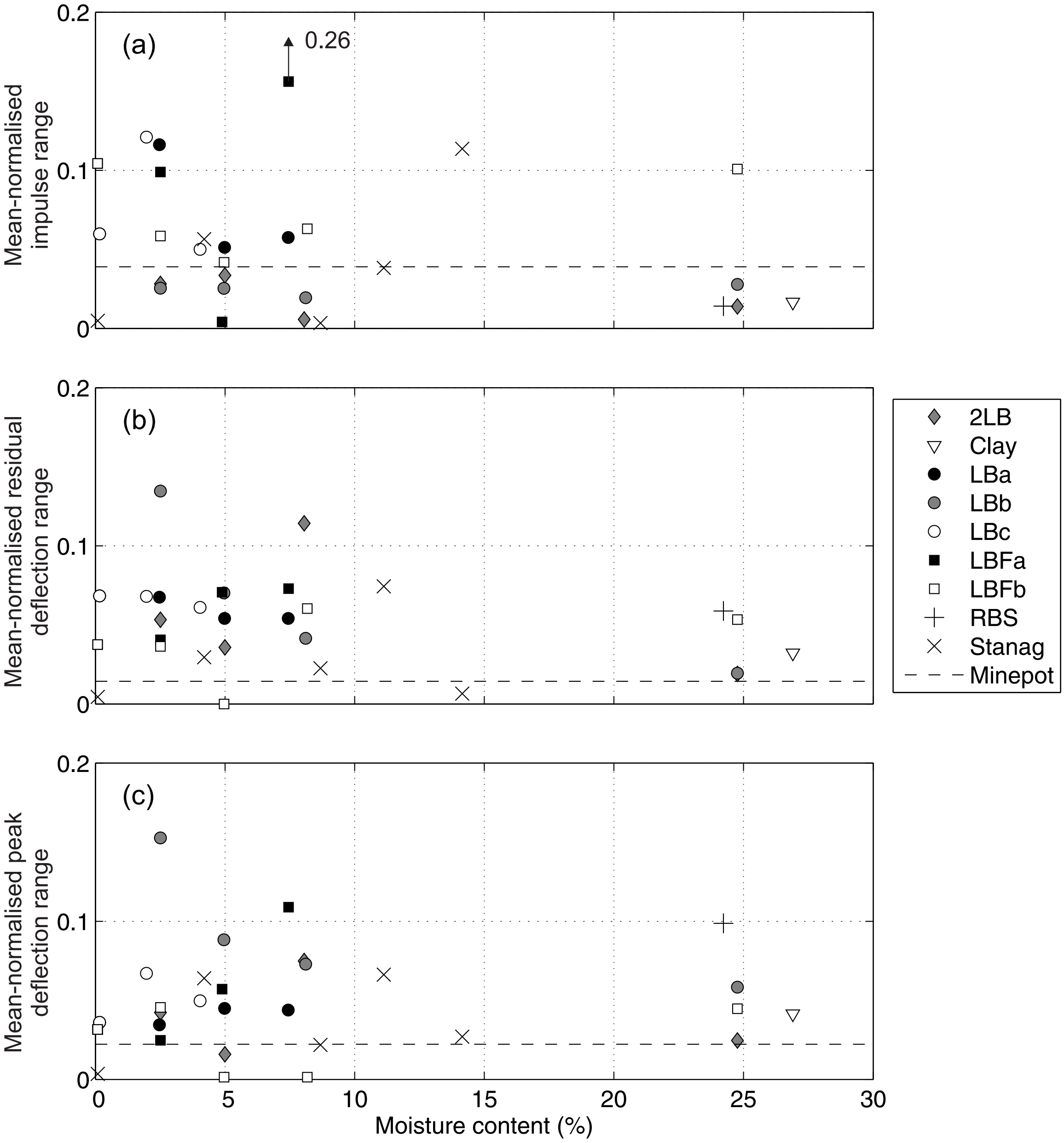

Figure 11: Moisture content versus the mean-normalised range of (a) impulse (b) residual deflection and (c) peak deflection

variation of impulse, again this is indicated in Fig. 12 with the LBb showing a high degree of repeatability in the geotechnical conditions and a low variation of impulse.

5. Conclusions

It has been shown that through careful soil preparation many soils can deliver a lower variation of impulse than seen when using the standard Minepot tests described in AEP-55 [12]. The maximum offset seen in any test was 26% away from the mean. 80% of the data generated lies within ±3.7% of the mean value for each test series.

The particle size distribution for cohesionless soils has been shown to be an indicator of the possible variation in impulse to be expected. This was shown previously [10, 11, 15] but has herein been shown to apply to a much greater range of soils. Currently the dataset for cohesive soils (Clay) is very small, but initial indications show a high degree of repeatability despite its relatively well graded particle size distribution.

Generally, well graded soils show a greater variation in the range of measured impulse for any given moisture content / bulk density combination, which could be due to local variations in density caused by the non-uniform nature of the soil. This trend however is not borne out in the plate deflection data where the range for most soil types is roughly equivalent. This illustrates the fact that despite very high control over the geotechnical conditions achieved in the presented work, if repeatability in the impulse generated in the tests is required a uniform soil should be utilised in the testing. This can be further refined to state that uniform cohesionless soils give repeatable results if bulk density is allowed to increase with moisture content. The most repeatable tests series in the reported data was that of the fully saturated Leighton Buzzard 14/25 sand (LB), which gave repeatable impulse and deflections, with the impulse variation being lower than seen in the Minepot tests.

This is of course postulated on the transfer of global impulse and takes no account of the localised loading effects which could be generated by changing between uniform and well graded

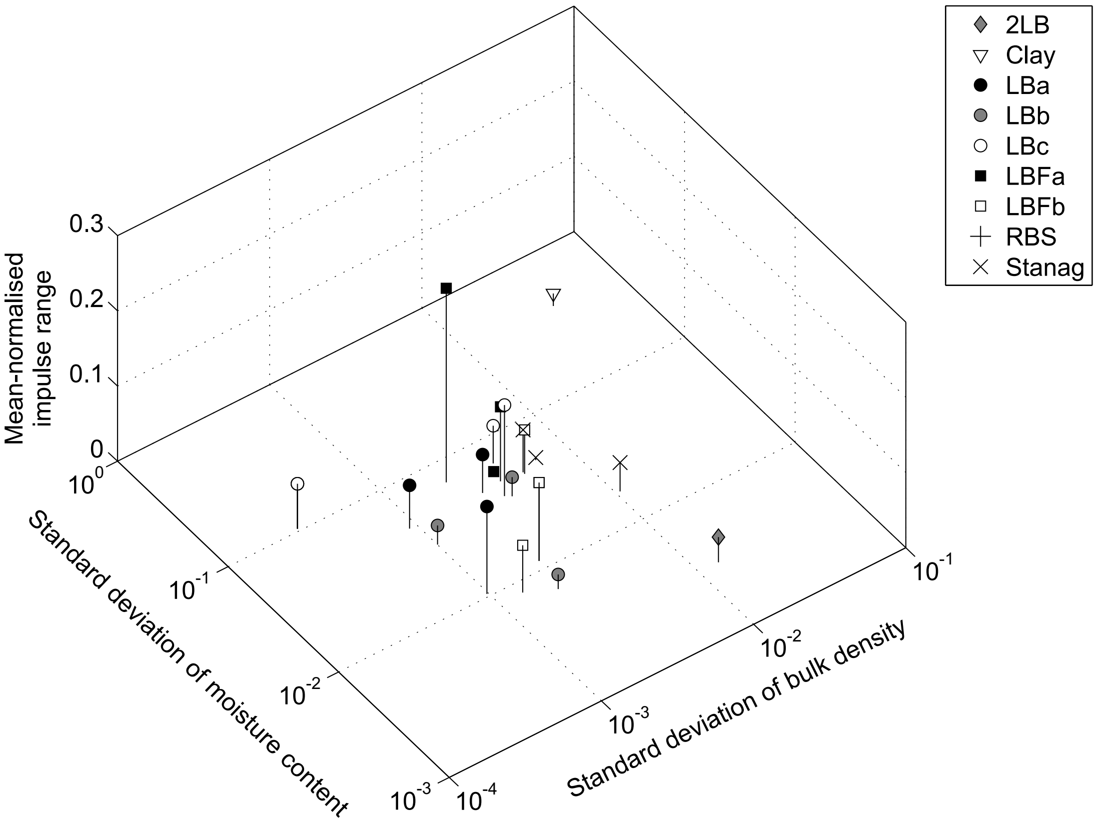

Figure 12: Controllability of geotechnical conditions versus the repeatability of the measured impulse

soils. This area of work is current being investigated in a separate project, details of which are published here [16].

Acknowledgements

The authors wish to thank the Defence Science and Technology Laboratory for funding the published work.

References

[1] Bergeron DM, Trembley JE. Canadian research to characterize mine blast output. *16th Int Sym on the Military Aspects of Blast and Shock, Oxford, UK*, 2000.

[2] Hlady SL. Effect of soil parameters on landmine blast. *18th Int Sym on the Military Aspects of Blast and Shock, Bad Reichenhall, Germany*, 2004.

[3] Pickering EG, Chung Kim Yuen S, Nurick, GN, Haw P. The response of quadrangular plates to buried charges. *Int J of Impact Eng*, 49:103–114, 2012.

[4] Fourney WL, Leiste U, Bonenberger R, Goodings DJ. Mechanism of loading on plates due to explosive detonation. *Int J on Blasting and Fragmentation*, 9(4):205–217, 2005.

[5] Anderson CE, Behner T, Weiss CE. Mine blast loading experiments. *Int J of Impact Eng*, 38(8-9):697–706, 2011.

[6] Fox DM, Huang X, Jung D, Fourney WL, Leiste U, Lee JS. The response of small scale rigid targets to shallow buried explosive detonations. *Int J of Impact Eng*, 38(11):882–891, 2011.

[7] Ehrgott JQ, Rhett RG, Akers SA, Rickman DD. Design and fabrication of an impulse measurement device to quantify the blast environment from a near-surface detonation in soil. *Experimental Techniques*, 35(3):51–62, 2011.

[8] Fox DM, Akers SA, Leiste UH, Fourney WL, Windham JE, Lee JS, Ehrgott JQ, Taylor LC. The effects of air filled voids and water content on the momentum transferred from a shallow buried explosive to a rigid target. *Intl J of Impact Eng*, 69(0):182–193, 2014.

[9] McShane GJ, Deshpande VS, Fleck NA. A laboratory-scale buried charge simulator. *Int J of Impact Eng*, 62:210–218, 2013.

[10] Clarke SD, Warren JA, Tyas A. The influence of soil density and moisture content on the impulse from shallow buried explosive charges. *Int Sym on Interaction of the Effects of Munitions with Structures, Seattle, US*, 2011.

[11] Clarke SD, Warren JA, Fay SD, Rigby SE, Tyas A. The role of geotechnical parameters on the impulse generated by buried charges. *22nd Int Sym on the Military Aspects of Blast and Shock, November 5-9, Bourges, France*, 2012.

[12] NATO. Procedures for evaluating the protection level of logistic and light armoured vehicles. *Allied Eng. Publication (AEP) 55*, Vol.2 (for Mine Threat), 2006.

[13] NATO. Protection levels for occupants of logistic and light armoured vehicles. *STANAG 4569*, 24th May, 2004.

[14] Cai Y, Yu H, Wanatowski D, Li X. Noncoaxial behavior of sand under various stress paths. *J of Geotechnical and Geoenvironmental Eng*, 139(8):1381–1395, 2013.

[15] Clarke SD, Fay SD, Tyas A, Warren J, Rigby S, Elgy I, Livesey R. Repeatability of buried charge testing. *23nd Int Sym on the Military Aspects of Blast and Shock, September 5-9, Oxford, UK*, 2014.

[16] Clarke SD, Fay SD, Warren JA, Tyas A, Rigby SE, Elgy I. A large scale experimental approach to the

measurement of spatially and temporally localised loading from the detonation of shallow-buried explosives. *Measurement Science and Technology*, 26:015001, 2015.